Strong nonreciprocal acoustic extinction and asymmetric audibility from spinning fluid scatterers

Yao-Ting Wang [1,2] Heedong Goh [1,3] Sander A. Mann [1] and Andrea Alù [1,3,4,*]

[1]*Photonics Initiative, Advanced Science Research Center, City University of New York, New York, New York 10031, USA*
[2]*Department of Photonics, National Sun Yat-Sen University, Kaohsiung 804201, Taiwan*
[3]*Department of Electrical and Computer Engineering, The University of Texas at Austin, Austin, Texas 78712, USA*
[4]*Physics Program, Graduate Center, City University of New York, New York, New York 10026, USA*

Lorentz reciprocity places important constraints on the response of systems to wave excitations, and surpassing these constraints is of both fundamental and applied interest. In the context of scattering, reciprocity requires that the total extinction of an object is identical when excited from opposite directions, regardless of the asymmetry of the scatterer. Here, we demonstrate that, by combining multiple scatterers that break time-reversal symmetry, this extinction symmetry can be largely violated. We consider spinning cylinders, demonstrating that nonreciprocity must be paired with broken parity symmetry to enable large extinction contrast. As a dramatic example, we show a system that strongly scatters when excited from one side, but it is cloaked for the opposite excitation. Our results pave the way for approaches to asymmetric audibility and scattering manipulation, and they may readily translate to other wave domains.

I. INTRODUCTION

Wave propagation in time-reversal symmetric systems obeys Lorentz reciprocity, a property formulated in acoustics by Lord Strutt [1] and later in electromagnetism by Lorentz [2]. Reciprocity guarantees symmetric wave propagation between two points in space: After changing the source and observer, the received wave amplitude and phase are identical, independent of the complexity of the environment. A consequence of reciprocity of particular interest in this paper is that the extinction cross-section, which describes the total power intercepted from an incident wave by a scatterer, must be identical for excitations from opposite directions [3], independent of how asymmetric the scatterer may be. As a byproduct, in the presence of material loss, asymmetric objects may have different scattering cross-sections when excited from opposite sides [4], but their total extinction (scattering plus absorption) must be identical, i.e., whatever difference in total scattered powers for excitation from opposite sides must be compensated by an opposite difference in absorption.

This extinction symmetry can be understood by considering the optical theorem, which dictates that the extinction cross-section σ_{ext} is proportional to the forward scattering amplitude $f(0)$, $\sigma_{\text{ext}} = 4\pi \text{Im}[f(0)]/k_0$, where k_0 is the wave number in the surrounding medium. Due to reciprocity, the amplitude and phase of forward transmission between source and observer must remain the same under their exchange; hence, if we place the object on the axis between source and observer, the forward scattering amplitude must also be independent of the incidence direction. As a byproduct, no passive object can be cloaked asymmetrically: Ideally, suppressing the scattering of an object from one side implies the

absence of scattering and absorption since absorption causes finite forward scattering in passive objects. Zero scattering and absorption, i.e., zero extinction, from one direction also requires zero extinction for excitations from the opposite side.

In this paper, we aim at breaking this general constraint by considering spinning acoustic scatterers that break time-reversal symmetry [3,5]. We demonstrate that, under proper conditions, this extinction symmetry can be largely violated, and unidirectional cloaking can be enabled. Reciprocity can be broken by incorporating a bias that is odd under time reversal, such as a magnetic field combined with gyromagnetic materials in optics. In acoustics, temporal modulation [6], nonlinear materials [7,8], and moving fluids [9–11] have been considered. Nonreciprocity combined with acoustic metamaterials has enabled forms of sound-matter interactions, including nonreciprocal Willis coupling [12–15] and topological acoustics [16–21]. In the following, we break reciprocity in acoustics to violate extinction symmetry by considering arrays of spinning cylinders [22–25]. We derive the scattering coefficients and define a polarizability tensor for small cylinders, showing that a spinning cylinder supports a peculiar quasistatic resonance at approximately half the angular velocity of the cylinder. We then use the optical theorem to flesh out the requirements to induce asymmetric extinction. Finally, we consider an array of three spinning cylinders to demonstrate extreme contrast in extinction for opposite excitation directions, resulting in strong scattering from one direction but cloaking from the opposite direction.

II. DIPOLE APPROXIMATION

In Fig. 1(a), we consider a system consisting of a rotating fluid with angular velocity Ω. Assuming that the fluid is inviscid, a fan generates a rotating fluid cylinder of radius r_s, while
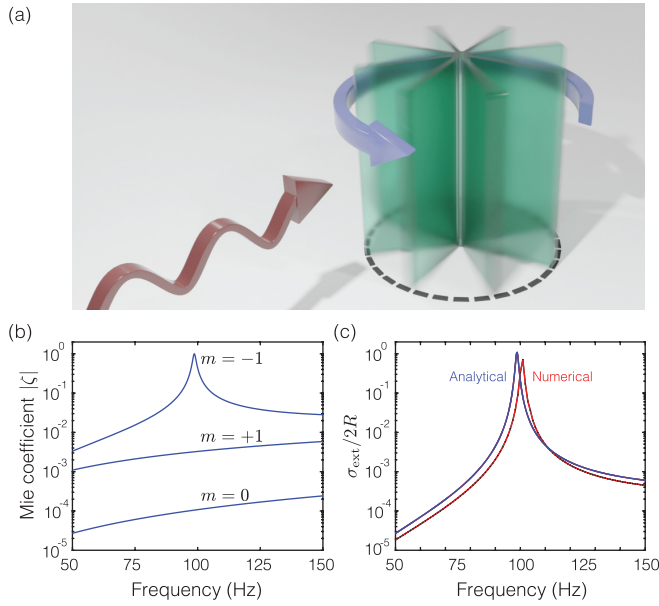
*aalu@gc.cuny.edu

(a)

(b)

(c)

FIG. 1. (a) Schematic geometry. The spinning fluid is generated by a rotating fan. (b) Mie scattering coefficients for the -1, 0, and 1 angular scattering orders for $\Omega = 2\pi \times 200$ rad/s. For a small spinning rod, the $m = \pm 1$ components are at least one order of magnitude larger than the others, with a clear resonance for one handedness. (c) $\sigma_{\text{ext}}^{\rightarrow}$ and $\sigma_{\text{ext}}^{\leftarrow}$ normalized to the geometrical cross-section, calculated using the dipole approximation, Mie theory, and numerically with COMSOL Multiphysics. The dipolar approximation (shown in blue) overlaps with Mie theory, as expected due to the dominance of the ± 1 angular channels. Importantly, $\sigma_{\text{ext}}^{\rightarrow}$ and $\sigma_{\text{ext}}^{\leftarrow}$ also overlap for all curves, indicating that, for a single spinning cylinder, the response is necessarily symmetric.

$\Omega = 0$ outside the spinning core. This geometry has been investigated experimentally in Ref. [13], where the expression for the azimuthal velocity $\mathbf{v}_\phi = \Omega r \hat{\mathbf{e}}_\phi$ was verified (see Supplemental Material [26] for possible implementations). We can derive the polarizability of a fluid rod rotating at speed Ω. The density and speed of sound are $\rho_s(\rho_0)$ and $c_s(c_0)$ for the cylinder and background medium, respectively. All angles in the following are defined between the corresponding vector direction and the x axis. From the linearized Navier-Stokes equations in the adiabatic approximation (implying no temperature exchange), for a cylindrical radius $r_s^2 \ll 2(c_0/\Omega)^2$, the Mie scattering coefficient for a rotating fluid cylinder reads (see Supplemental Material [26])

$$\zeta_m = -\frac{\lambda_m \rho_0 R_m(\lambda_m r_s) J_m(k_0 r_s) - k_0 \rho_s J_m(\lambda_m r_s) J'_m(k_0 r_s)}{\lambda_m \rho_0 R_m(\lambda_m r_s) H_m(k_0 r_s) - k_0 \rho_s J_m(\lambda_m r_s) H'_m(k_0 r_s)}. \quad (1)$$

Here, $k_0 = \omega/c_0$, with ω being the angular frequency of the impinging wave, $\lambda_m^2 = (M^2 - 4\Omega^2)/c_s^2$, $M = (\omega - m\Omega)$, and the auxiliary function $R_m(\lambda_m r_s)$ is given by

$$R_m(\lambda_m r_s) = \frac{\omega}{M^2 - 4\Omega^2}\left[MJ'_m(\lambda_m r_s) - 2m\Omega \frac{J_m(\lambda_m r_s)}{\lambda_m r_s}\right], \quad (2)$$

where $J_m(z)$ is the Bessel function of the first kind. It is worth noting that, although the choice of boundary conditions alters the expression of Eq. (2), it does not significantly affect

the scattering features within in the subwavelength regime of interest (see Sec. 2 in the Supplemental Material [26] for more details). Figure 1(b) shows the dispersion of the first three Mie coefficients. The zeroth-order Mie coefficient is approximately two orders of magnitude smaller than the other two within the targeted frequency range, indicating that the system is dominated by the dipolar response if the cylinder radius is subwavelength. As a result, in the following, we consider only the dipolar response, which can be conveniently described through the polarizability tensor $\bar{\bar{\alpha}}$, relating the induced dipole moment vector D to the velocity field v of the impinging wave (see Supplemental Material [26]):

$$\begin{bmatrix} D_x \\ D_y \end{bmatrix} = \bar{\bar{\alpha}} \begin{bmatrix} v_x \\ v_y \end{bmatrix} = \begin{bmatrix} \alpha_{xx} & -\alpha_{xy} \\ \alpha_{xy} & \alpha_{xx} \end{bmatrix} \begin{bmatrix} v_x \\ v_y \end{bmatrix}$$

$$= \frac{4i}{\omega^2} \begin{bmatrix} \zeta_1 + \zeta_{-1} & -i(\zeta_1 - \zeta_{-1}) \\ i(\zeta_1 - \zeta_{-1}) & \zeta_1 + \zeta_{-1} \end{bmatrix} \begin{bmatrix} v_x \\ v_y \end{bmatrix}. \quad (3)$$

Note that $\bar{\bar{\alpha}}(\Omega) \neq \bar{\bar{\alpha}}(\Omega)^T$ (the superscript T represents the transpose of a matrix), indicating that the cylinder violates reciprocity [27]. As the cylinder itself is symmetric, the off-diagonal terms arise due to the rotation, and indeed, it is straightforward to verify that, under a time-reversal operation, the tensor is symmetric: $\bar{\bar{\alpha}}(\Omega) = \bar{\bar{\alpha}}(-\Omega)^T$.

In the long-wavelength limit and under the assumption that the cylinder and background media are the same, we obtain the interesting result:

$$\zeta_{\pm 1} = \frac{-\Omega}{\Omega \pm (2\omega \pm \Omega)(4i/\pi k_0^2 r_s^2)}. \quad (4)$$

Equation (4) indicates that a quasistatic resonance can arise without the need for impedance mismatch at the cylinder boundary. This rotation-induced resonance has frequency ω_{res}, obeying

$$4\omega_{\text{res}}^2 = \Omega^2 \left[1 - \frac{\pi^2}{16}\left(\frac{\omega_{\text{res}} r_s}{c_0}\right)^4\right], \quad (5)$$

derived by requiring that the real part of the denominator of $\zeta_{\pm 1}$ vanishes. Equation (5) can be further approximated using $(\Omega r_s/c_0)^4 \ll 1$, which results in $\omega_{\text{res}} \approx \Omega/2$ (see Supplemental Material [26]). Hence, despite being made of the same material as the background, a small spinning cylinder strongly scatters at frequencies half the angular spinning frequency. In other words, the rotation of a fluid drastically changes the material effective properties around half the spinning frequency in the quasistatic regime. The result is consistent with the numerical calculations in Fig. 1(b), which highlight a strong resonant response for ζ_{-1} at 100 Hz, due to the rotation. The large contrast between ζ_{-1} and ζ_{+1} is another manifestation of broken symmetry due to spin. As may be expected, the angular-order spinning against the fluid rotation is the one being amplified, as it feels a stronger Doppler shift due to the faster relative velocity.

III. ACOUSTIC EXTINCTION CONTRAST

Under excitation with an incident plane wave, Fig. 1(c) shows the left-to-right and right-to-left extinction cross-section ($\sigma_{\text{ext}}^{\rightarrow}$ and $\sigma_{\text{ext}}^{\leftarrow}$) calculated through the dipole
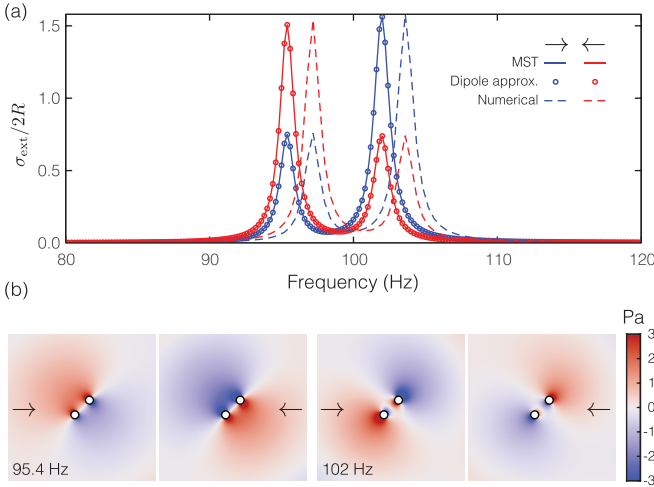
FIG. 2. (a) $\sigma_{\text{ext}}^{\rightarrow}$ and $\sigma_{\text{ext}}^{\leftarrow}$ of two spinning cylinders rotating in opposite directions. We find two nondegenerate resonant peaks for either direction of incidence. (b) Scattered field profiles at the resonances, as calculated by the dipole approximation. A comparison with COMSOL is presented in the Supplemental Material [26].

approximation (DA), Mie scattering theory, and numerically with COMSOL Multiphysics. Despite breaking time-reversal symmetry, there is no sign of nonreciprocity: The curves for $\sigma_{\text{ext}}^{\rightarrow}$ and $\sigma_{\text{ext}}^{\leftarrow}$ cannot be distinguished. This is because a single spinning object is back to its original state after $2\pi/\Omega$ seconds, which only causes a phase difference in the scattered field for opposite excitations, preserving the same scattering amplitude. To achieve asymmetric extinction, we need to also break parity symmetry; hence, at least two spinning cylinders (or an asymmetric geometry) are required. Next, we consider N rotating cylinders located at separate positions at a distance $r_{jk} = |\mathbf{r}_j - \mathbf{r}_k|$. Their dressed dipole moments can be written as

$$
\begin{bmatrix} D_x^{(j)} \\ D_y^{(j)} \end{bmatrix} = \bar{\bar{\alpha}}_j \left(\begin{bmatrix} v_{0x}^{(j)} \\ v_{0y}^{(j)} \end{bmatrix} + \sum_{k=1, k \neq j}^{N} \bar{\bar{G}}_{jk} \begin{bmatrix} D_x^{(k)} \\ D_y^{(k)} \end{bmatrix} \right). \quad (6)
$$

Here, the normalized velocity fields at position j equals $\exp[i\eta_j(\phi_{\text{inc}})][\cos\phi_{\text{inc}}, \sin\phi_{\text{inc}}]^T$, where the phase $\eta_j = k_0 r_j \cos(\phi_{\text{inc}} - \phi_{r_1})$, and ϕ_{inc} is the incident angle. The incident pressure amplitude is assumed to be unity. The Green's tensor $\bar{\bar{G}}_{jk}$ yields the velocity field of one dipole at the location of the other one and, in the long-wavelength approximation ($k_0 r_{jk} \ll 1$), is given by (see Supplemental Material [26])

$$
\bar{\bar{G}}_{jk} = \frac{i\omega^2}{8} H_2(k_0 r_{jk}) \begin{bmatrix} \cos 2\phi_{jk} & \sin 2\phi_{jk} \\ \sin 2\phi_{jk} & -\cos 2\phi_{jk} \end{bmatrix}, \quad (7)
$$

where $H_2(k_0 r_{jk})$ denotes the Hankel function of the first kind.

We now specialize this formulation to the case of two counterrotating cylinders, as shown in the inset of Fig. 2(a). The angle ϕ_{jk}, with $j, k = 1, 2$ and $j \neq k$, represents the angle between the distance vector $\mathbf{r}_{jk} = \mathbf{r}_j - \mathbf{r}_k$ and the x axis. Note that the choice of r_{jk} cannot be too small, to avoid that higher-order modes, neglected by the DA, become significant in the near-field coupling. In this scenario, multiple scattering

theory (MST) [28] may be exploited to incorporate higher-order angular modes.

Once the dipole moments are obtained, the total far-field scattered wave p_{sca} asymptotically approaches $f_{\text{tot}}(\phi)\exp(ik_0 r)/\sqrt{r}$ as $r \to \infty$, with

$$
f_{\text{tot}}(\phi) = \frac{\omega^2}{4} \exp\left(-i\frac{3\pi}{4}\right) \sqrt{\frac{2}{\pi k_0}}
$$

$$
\times \sum_{j=1}^{N} \left[D_x^{(j)} \cos\phi + D_y^{(j)} \sin\phi \right] \exp[-i\psi_j(\phi)]. \quad (8)
$$

Here, $\psi_j(\phi) = k_0 r_j \cos(\phi_{r_j} - \phi)$ denotes the phase correction from position j to the origin (see Supplemental Material [26]). To verify our theory, we compare the results of $\sigma_{\text{ext}}^{\rightarrow}$ and $\sigma_{\text{ext}}^{\leftarrow}$ calculated from Eq. (8), MST, and COMSOL for $r_s = 5$ cm, $\Omega = 2\pi \times 200$ rad/s, and an angle $\phi_{r_1} = 45°$ between the cylinders. The spinning cylinders and background medium are both considered to be air with density of 1.21 kg/m^3 and sound speed of 343 m/s. Figure 2(a) shows the extinction cross-sections for all three methods. There is a 2 Hz frequency shift between numerical and analytical results due to the DA in Eq. (1). However, apart from this shift, the cross-sections are in excellent agreement.

In contrast with the result for a single cylinder, we observe strong asymmetry at 95.4 and 102 Hz (97.2 and 103.6 Hz for the COMSOL results). Hence, these spectra demonstrate violation of the extinction symmetry because of breaking both reciprocity and parity symmetry. This effect can also be observed in the field patterns of Fig. 2(b), with a significant difference in the scattered field when excited from $-x$ or $+x$ (see Supplemental Material [26]).

To unveil the underlying physics behind the nonreciprocal extinction phenomenon, we analytically derived the difference between $\sigma_{\text{ext}}^{\rightarrow}$ and $\sigma_{\text{ext}}^{\leftarrow}$ based on the optical theorem (see Supplemental Material [26]) [29]:

$$
\Delta\sigma_{\text{ext}} = -2\sqrt{\pi/k_0}[\text{Re}\{\Delta f_{\text{tot}}\} - \text{Im}\{\Delta f_{\text{tot}}\}], \quad (9)
$$

where Δf_{tot} is the contrast of total scattering amplitudes. For a structure made of two cylinders spinning in the same direction, Δf_{tot} vanishes when $k_0 d \ll 1$; in contrast, for opposite spinning directions, the difference of $+x$ and $-x$ scattering amplitudes is (see Supplemental Material [26])

$$
\Delta f_{\text{tot}} = f_{\text{tot}}(0) - f_{\text{tot}}(\pi)
$$

$$
= \sqrt{\frac{8}{\pi k_0}} \frac{\omega^2 e^{-i\pi/4} \alpha_{xx} \alpha_{xy} Q \sin 2\phi_{r_1} \sin(2k_0 r_1 \cos\phi_{r_1})}{(\alpha_{xx}^2 + \alpha_{xy}^2)^2 Q^4 - 2(\alpha_{xx}^2 - \alpha_{xy}^2)Q^2 + 1}, \quad (10)
$$

where $Q = i\omega^2 H_2(k_0 d)/8$. From a symmetry standpoint, a pair of identical spinning cylinders obeys C_2 symmetry. Thus, incident waves from opposite directions see the same geometry and induce the same scattered fields. However, a pair of counterrotating cylinders breaks C_2 symmetry, giving rise to an extinction cross-section contrast from opposite directions
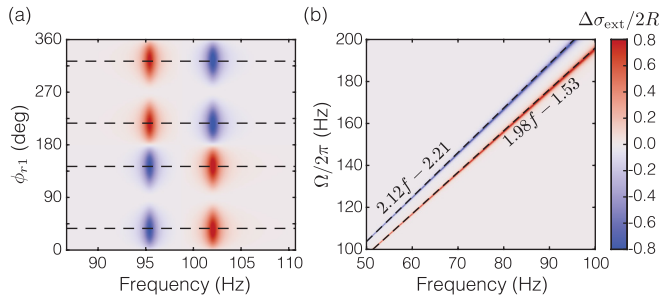
FIG. 3. (a) σ_{ext} difference $\Delta\sigma_{\mathrm{ext}} = \sigma_{\mathrm{ext}}^{\rightarrow} - \sigma_{\mathrm{ext}}^{\leftarrow}$ in terms of frequency and ϕ_{r_1}. (b) σ_{ext} contrast in terms of excitation frequency and spinning frequency Ω. The two maxima move further apart for increasing Ω, like Zeeman splitting.

but only for appropriate geometrical configurations. For example, Eq. (10) indicates that Δf_{tot} vanishes as $\phi_{r_1} = 0$ and $\pi/2$, for which $\sigma_{\mathrm{ext}}^{\rightarrow}$ and $\sigma_{\mathrm{ext}}^{\leftarrow}$ become identical because of restored symmetry with respect to the excitation direction. We show the contrast in extinction in Figs. 3(a) and 3(b), as a function of orientation and spinning velocity. The extinction contrast oscillates as the angle ϕ_{r_1} varies from 0° to 360°, reaching its maximum values when $\phi_{r_1} \approx 37°$, 143°, 217°, and 323°, consistent with Eq. (9). A 180° rotation results in the same extinction contrast, as expected due to symmetry considerations. As may be intuitively expected, these angles are close to the diagonal orientations with respect to the excitation. In fact, within the DA, the orientation for maximal contrast falls on the diagonal in the limit of $d = 0$; the slight deviation from the diagonal stems from retardation effects due to the nonzero separation.

As shown in Fig. 3(b), the dependence of the extinction difference is linearly proportional to the rotation velocity Ω within this frequency range. The difference between the contrast maxima and minima, obtained by fitting the linear dispersion is $\Delta f = 0.034\Omega/2\pi - 0.266$, inducing a Zeeman-like splitting in resonances induced by the spin, analogous to gyromagnetic phenomena [22], where the rotation velocity replaces the magnetic field strength.

IV. STRONG ACOUSTIC EXTINCTION CONTRAST

By increasing the number of cylinders, larger extinction contrast can be achieved. While it is cumbersome or even intractable to derive analytic expressions as the number of cylinders increases, Eq. (6) can readily be solved analytically to obtain the corresponding far-field response via Eq. (8). As shown in the inset of Fig. 4(a), we consider two counterclockwise-rotating rods located at $(1.6, 2)r_s$ and $(-1.6, 2)r_s$ and one clockwise-rotating rod located at $(-6.5, 6.5)r_s/\sqrt{2}$, where the radius of rods r_s is now 6 cm. These locations have been determined through a geometrical parameter sweep, and they may be further optimized through inverse design techniques, particularly when more cylinders are considered. The $\sigma_{\mathrm{ext}}^{\rightarrow}$ and $\sigma_{\mathrm{ext}}^{\leftarrow}$ spectra for this configuration calculated with the DA are shown in Fig. 4(a) with dashed lines. At 98.150 Hz, a strong extinction contrast is observed, with $\sigma_{\mathrm{ext}}^{\rightarrow} > 10$ times larger than $\sigma_{\mathrm{ext}}^{\leftarrow}$. To verify that this
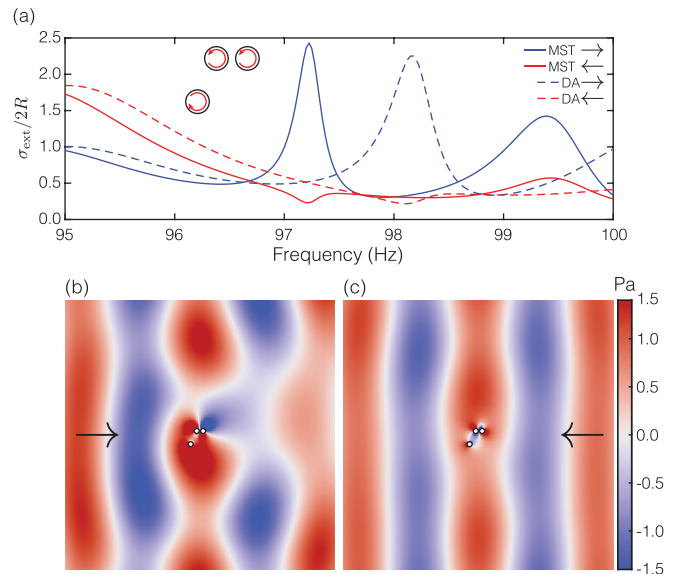

FIG. 4. (a) Extinction cross-section spectra of the array depicted schematically in the inset, composed of three spinning rods. (b) and (c) The total field profiles are illustrated for the two directions of incidence, demonstrating strong extinction for excitation from the left, while nearly ideal cloaking for incidence from the right.

contrast persists in the presence of higher-order modes, we also show results calculated with MST (solid lines). While incorporating higher-order modes induces a small frequency shift and narrower linewidths, the large contrast remains unchanged. The slight discrepancy arises because the cylinders are in close proximity (see Supplemental Material [26] for the spectra calculated with COMSOL). The asymmetry in extinction can also clearly be observed in the field patterns around the rotating cylinders [Figs. 4(b) and 4(c)]. Strong scattering occurs when the cylinders are excited from the left [Fig. 4(b)], while the incident plane wave propagates almost unperturbed when excited from the right [Fig. 4(c)], realizing a unidirectional cloaking response that largely violates the extinction symmetry obeyed by reciprocal scatterers.

V. CONCLUDING REMARKS

In this paper, we have investigated large nonreciprocal extinction in arrays of spinning cylinders. First, we have unveiled an exotic nonreciprocal quasistatic resonance arising at approximately half the spinning angular velocity. However, for a single cylinder $\sigma_{\mathrm{ext}}^{\rightarrow}$ and $\sigma_{\mathrm{ext}}^{\leftarrow}$ remain identical. This is to be expected because, despite spinning, a single cylinder does not break parity symmetry. Instead, two cylinders with opposite rotation directions and broken parity can largely break extinction symmetry. The underlying physics is analogous to Zeeman splitting in atomic systems in the presence of a magnetic field, with the distance between maximal extinction differences increasing linearly with the spin velocity Ω. Finally, we showed a configuration of three spinning cylinders supporting unidirectional transparency. Such asymmetric audibility may have various applications, such as in noise

control and scattering manipulation. Given the universality of reciprocity and time-reversal symmetry in wave systems, we expect that our results can readily translate to other fields, including opportunities for asymmetric visibility [30].

[1] J. W. Strutt, Proc. Lond. Math. Soc. **s1-4**, 357 (1871).

[2] H. A. Lorentz, Amsterdammer Akademie der Wetenschappen **4**, 176 (1896).

[3] D. Sounas and A. Alù, Opt. Lett. **39**, 4053 (2014).

[4] M. Goodarzi and T. Pakizeh, Opt. Lett. **44**, 2212 (2019).

[5] Y.-T. Wang, J. Acoust. Soc. Am. **148**, 1259 (2020).

[6] R. Fleury, D. L. Sounas, and A. Alù, Phys. Rev. B **91**, 174306 (2015).

[7] B. Liang, B. Yuan, and J. C. Cheng, Phys. Rev. Lett. **103**, 104301 (2009).

[8] B. Liang, X. S. Guo, J. Tu, and D. Zhang, Nat. Mater. **9**, 989 (2010).

[9] P. M. Morse and K. U. Ingard, *Theoretical Acoustics* (McGraw-Hill, New York, 1968).

[10] O. A. Godin, Wave Motion **25**, 143 (1997).

[11] R. Fleury, D. L. Sounas, C. F. Sieck, M. R. Haberman, and A. Alù, Science **343**, 516 (2014).

[12] L. Quan, Y. Ra'di, D. L. Sounas, and A. Alù, Phys. Rev. Lett. **120**, 254301 (2018).

[13] L. Quan, S. Yves, Y. Peng, H. Esfahlani, and A. Alù, Nat. Comm. **12**, 2615 (2021).

[14] H. Esfahlani, Y. Mazor, and A. Alù, Phys. Rev. B **103**, 054306 (2021).

[15] C. Olivier, G. Poignand, M. Malléjac, V. Romero-García, G. Penelet, Au. Merkel, D. Torrent, J. Li, J. Christensen, and J.-P. Groby, Phys. Rev. B **104**, 184109 (2021).

[16] X. Ni, C. He, X. Sun, X. Liu, M. Lu, L. Feng, and Y. Chen, New J. Phys. **17**, 053016 (2015).

[17] Z. Yang, F. Gao, X. Shi, X. Lin, Z. Gao, Y. Chong, and B. Zhang, Phys. Rev. Lett. **114**, 114301 (2015).

[18] P. Wang, L. Lu, and K. Bertoldi, Phys. Rev. Lett. **115**, 104302 (2015).

[19] Z.-G. Chen and Y. Wu, Phys. Rev. Appl. **5**, 054021 (2016).

[20] A. B. Khanikaev, R. Fleury, S. H. Mousavi, and A. Alù, Nat. Commun. **6**, 8260 (2015).

[21] L. M. Nash, D. Kleckner, A. Read, V. Vitelli, A. M. Turner, and T. M. Irvine, Proc. Natl. Acad. Sci. USA **112**, 14495 (2015).

[22] D. Zhao, Y.-T. Wang, K.-H. Fung, Z.-Q. Zhang, and C. T. Chan, Phys. Rev. B **101**, 054107 (2020).

[23] M. Farhat, S. Guenneau, A. Alù, and Y. Wu, Phys. Rev. B **101**, 174111 (2020).

[24] M. Farhat, P.-Y. Chen, M. Amin, A. Alù, and Y. Wu, Phys. Rev. B **104**, L060104 (2021).

[25] N. Wang, R.-Y. Zhang, and C. T. Chan, Phys. Rev. Appl. **15**, 024034 (2021).

[26] See Supplemental Material at http://link.aps.org/supplemental/10.1103/PhysRevB.108.165129 for mathematical details on the derivations and additional comsol verifications on scattered field patterns.

[27] I. Sersic, C. Trambilangana, T. Kampfrath, and A. F. Koenderink, Phys. Rev. B **83**, 245102 (2011).

[28] L.-M. Li and Z.-Q. Zhang, Phys. Rev. B **58**, 9587 (1998) and the references therein.

[29] P. A. Maurone and T. K. Lim, Am. J. Phys. **51**, 856 (1983).

[30] S. Alyones, C. W. Bruce, M. Granado, and A. V. Jelinek, Appl. Optics **54**, 12 (2015).